Journal of Power Sources 241 (2013) 6–11

Contents lists available at SciVerse ScienceDirect

Journal of Power Sources

journal homepage: www.elsevier.com/locate/jpowsour

Phenol–formaldehyde carbon with ordered/disordered bimodal mesoporous structure as high-performance electrode materials for supercapacitors

Tingwei Cai, Min Zhou, Guangshuai Han, Shiyou Guan*

School of Materials Science and Engineering, East China University of Science and Technology, Mei Long Road 130, Shanghai 200237, PR China

HIGHLIGHTS

- The BMC with ordered/disordered pore structure was synthesized.
- The BMC possesses good supercapacitive properties.
- The BMC exhibits specific capacitance of 344 F g^{-1} at 0.1 A g^{-1}.
- The BMC shows excellent cycling stability after 10,000 cycles.

ARTICLE INFO

Article history:
Received 25 February 2013
Received in revised form
9 April 2013
Accepted 24 April 2013
Available online 30 April 2013

Keywords:
Bimodal mesoporous
Chemical modification
Phenol–formaldehyde carbon
Supercapacitor

ABSTRACT

A novel phenol–formaldehyde carbon with ordered/disordered bimodal mesoporous structure is synthesized by the facile evaporation induced self-assembly strategy under a basic aqueous condition with SiO_2 particles as template. The prepared bimodal mesoporous carbons (BMCs) are composed of ordered mesoporous and disordered mesoporous with diameter of about 3.5 nm and 7.0 nm, respectively. They can be employed as supercapacitor electrodes in H_2SO_4 aqueous electrolyte after the simple acid-treatment. BMC exhibits an exceptional specific capacitance of 344 F g^{-1} at the current density of 0.1 A g^{-1}, although it has a relatively low surface area of 722 m^2 g^{-1}. And the BMC electrode displays an excellent cycling stability over 10,000 cycles.

1. Introduction

In response to the need of modern society and emerging ecological, the development of new electrochemical energy storage/convert systems with high-performance, low-cost and environmentally friendliness is more and more essential [1,2]. Supercapacitors and lithium-ion batteries are considered to be important energy storage devices. As compared with lithium-ion batteries, supercapacitors possess much longer cycle life, higher power densities, shorter charge/discharge time, but relatively lower energy densities [3–6]. Electrical double-layer capacitors (EDLCs) are currently commercially available supercapacitors due to their higher power density and longer life time than faradaic pseudocapacitors [7,8]. Porous carbons, especially activated carbons, are regarded as first candidate electrode materials for EDLCs because of their stable physicochemical properties, high surface area, tunable structures, good conductivities and low-cost. As we know, the surface area of porous carbons can reach 3000 m^2 g^{-1}, but only about 10–20% of the "theoretical" capacitance is observed due to the presence of micropores that are inaccessible by the electrolyte [9,10].

In order to achieve ideal EDLCs with high energy density and power density, numerous efforts have been devoted to the synthesis of tailored porous carbon materials [11–14], and the activated or ordered mesoporous carbons have been widely studied [15–18]. Although ordered mesoporous carbons (OMCs) possess the controllable pore sizes and structures, which are more favorable for fast ionic transport than the pore networks in the disordered microporous carbons, their mesoporous channels (3–6 nm) cannot fulfill high-rate EDLCs applications at high current densities, where ionic transport with the pores is hindered and thus the full electrochemically active surface area is often not accessed [19,20].

Recently, considering their unique pores structures, bimodal mesoporous carbons (BMCs) have gained increasing interest as the

* Corresponding author. Tel./fax: +86 21 64251509.
E-mail address: syguan@ecust.edu.cn (S. Guan).

0378-7753/$ – see front matter © 2013 Elsevier B.V. All rights reserved.
http://dx.doi.org/10.1016/j.jpowsour.2013.04.112

electrode materials for supercapacitors to fit the request of high power and energy density [19–25]. Unfortunately, the pores of BMCs with diameter less than 2 nm are not beneficial for fast ion diffusion in electrodes [22]. Meanwhile, the pores larger than 20 nm decrease the specific surface area leading to low specific capacitance [24]. Therefore, it is of significance to readily and effectively synthesize BMCs with pore size distribution of about 3 nm and 10 nm, which cannot only provide large specific surface area, high specific capacitance but also improve the ion diffusion to electrodes at high-rate.

Herein, a novel phenol–formaldehyde carbon with ordered/disordered bimodal mesoporous structure (3.5 and 7.0 nm) and high surface area (722 $m^2\ g^{-1}$) is synthesized for the first time by the facile evaporation induced self-assembly strategy (EISA) under a basic aqueous condition using SiO_2 particles as template [23,26–28]. Through the connection to the disordered mesoporous (7.0 nm), the ordered mesoporous (3.5 nm) can provide enough channels for the transportation of the electrolyte from the surface into the inside disordered pores of electrode particles. Thus, BMCs can obtain high surface area, specific capacitance. Meanwhile, at high current densities, the disordered mesoporous can still supply efficient electrolyte diffusion pathways for their larger pore size leading to excellent rate capability. After a simple modification by acid-treatment [29,30], the BMCs electrodes exhibit an outstanding maximum specific capacitance of 344 F g^{-1} at the current density of 0.1 A g^{-1}, and maintain 63% (216 F g^{-1}) at 10 A g^{-1}. The excellent stability of less than 1% decay in specific capacitance after 10,000 cycles is also obtained. To the best of our knowledge, we firstly demonstrate bimodal mesoporous carbon with ordered/disordered mesoporous structure as electrodes for supercapacitors, and the outstanding performances in all of the important aspects are achieved.

2. Experimental section

Triblock copolymer Pluronic F127 (Mw = 12,600, $EO_{106}PO_{70}EO_{106}$) was purchased from Aldrich Chemical Inc. used as soft template and silica particles used as hard template were get from Evonik (A150, GER). Other chemicals were purchased from Shanghai Chemical Corp.. All chemicals were used as received without any further purification. Deionized water was used in all experiments.

2.1. Synthesis of resol precursor

A soluble low molecular weight polymer (Mw = ~500) derived from resol was prepared by basic polymerization. Typically, phenol (6.1 g, 65.0 mmol) was melted at 40–42 °C before 20% NaOH (aq: 1.3 g, 6.5 mmol) was added slowly over 10 min with stirring. Formalin (37 wt.%, 10.5 g) containing formaldehyde (130.0 mmol) was added dropwise, and the reaction mixture was stirred at 70 °C for 1 h. After cooling the mixture to room temperature, the pH of the reaction mixture was adjusted to neutral (7.0) using HCl (0.6 M) solution. Water was then removed under vaccum below 50 °C. The final product (Mw <500 measured by GPC) was redissolved in ethanol (63.6 g) and the salt NaCl was filtered before use.

2.2. Synthesis of mesoporous carbons

BMC was prepared by a facile evaporation induced self-assembly strategy under a basic aqueous condition [26–28]. In a typical preparation, F127 (0.3 g) was dissolved in ethanol (4.5 g), and then resol precursors in an ethanol solution (5.07 g) containing phenol (0.4 g) and formaldehyde (0.26 g) was added under stirring. Meanwhile, SiO_2 particles (0.26 g) were added into the reaction mixture to form a viscous, homogeneous solution after stirring for 30 min which was poured into dishes to evaporate ethanol at room temperature for 8 h. Then the products were heated in an oven at 120 °C for 24 h followed by carbonization in a tube oven under nitrogen at 800 °C for 2 h. At last, the products were treated by with NaOH solution (2 M) at 80 °C for 2 h to remove the SiO_2 particles followed by washed and dried at 80 °C for 12 h before use. Meanwhile, ordered mesoporous carbon (OMC) and disordered mesoporous carbon (DMC) were also synthesized by almost the same process without the use of SiO_2 particles and F127, respectively.

2.3. Chemical modification of mesoporous carbons

Mesoporous carbons (BMC, OMC, DMC) were chemically modified using HNO_3 solution. Briefly, the product (0.1 g) was suspended in HNO_3 (68 wt.%, 10 mL) and then refluxed at 65 °C for 1 h. After the mixture was cooled down to room temperature, it was filtered and washed with deionized water until the pH value of the filtrate was around 7. Then the product was dried at 80 °C for 12 h in air.

2.4. Electrochemical measurements

The electrochemical measurements were performed with an electrochemical analyzer system (CHI 660D, Chenhua, Shanghai, China) under ambient conditions in H_2SO_4 aqueous solution (1 M), using a three-electrode system. The working electrode was prepared by mixing 85 wt.% of the synthesized mesoporous phenol–formaldehyde carbon (BMC, OMC and DMC), 10 wt.% acetylene black and 5 wt.% polytetrafluoroethylene (PTFE). Briefly, the resulting paste was pressed on a titanium gauze at 5 MPa for 40 s. The counter and the reference electrodes were platinum wire and Ag/AgCl electrode (3 M KCl solution), respectively. The specific capacitances were calculated from the slopes of the charge/discharge curves.

2.5. Characterization of materials

Powder X-ray diffraction (XRD) pattern was obtained on a D/MAX 2550VB/PC diffractometer (Rigaku, Japan) using Cu Kα radiation ($\lambda = 0.154$ nm) at a scanning speed of 0.5° min^{-1} from 0.5° to 5°. The surface morphology and pore size were examined by transmission electron microscopy (TEM, JEM-2100 JEOL, Japan). The chemical composition of the samples was analyzed by Fourier transformation infrared spectroscopy (FTIR) using a Nicolet 5700 (Thermo Electron Crop., USA). The surface area of the samples was measured by the standard Brunauer–Emmett–Teller method (BET) using a NOVA 4200e (Quantachrome, USA) instrument.

3. Results and discussion

3.1. Microstructure characterizations

The general preparation of BMC can be briefly described by the following process as shown in Fig. 1. BMCs with ordered/disordered mesoporous structure were synthesized from the co-assembly of the triblock copolymer Pluronic F127, resol, and SiO_2 particles, followed by thermopolymerization and carbonization, successively. At last, the SiO_2 particles were etched away by alkaline wash. Ordered mesoporous carbon (OMC) and disordered mesoporous carbon (DMC) were also synthesized by almost the same process without the use of SiO_2 particles and F127, respectively. It should be noted that the alkaline wash was not carried out on OMC. According to our previous work [31], mesoporous phenol–formaldehyde carbon did not show well electrochemical properties due to its bad wettability with the aqueous electrolyte, but it could be obviously

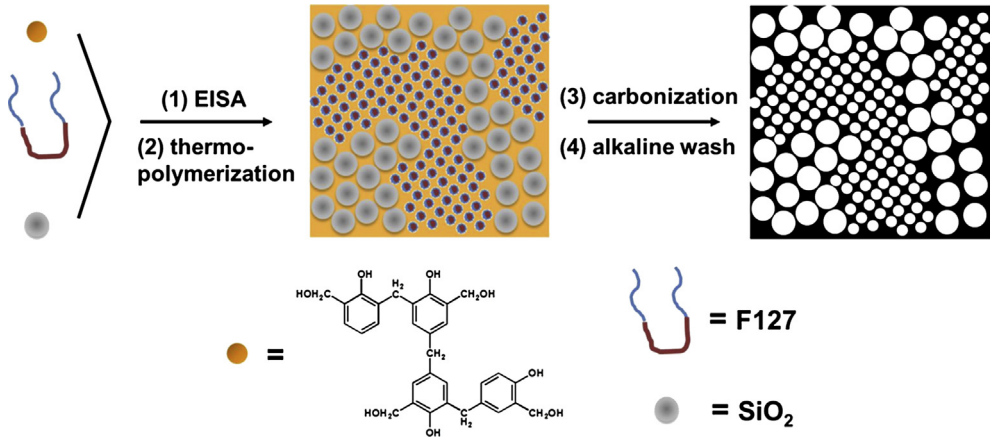

Fig. 1. Schematic illustration for the preparation of BMC with bimodal mesoporous structure.

improved by acid-treatment. In this work, a simple acid-treatment was also carried out on these phenol–formaldehyde carbons before characterizations and electrochemical tests.

The small-angle XRD pattern of BMC shows only a broad diffraction peak at 2θ around 0.8° instead of a strong peak from ordered mesoporous structure of OMC [27], indicating the poor long-range order of BMC (Fig. 2). In the XRD of DMC, there are even no obvious peaks appeared, which means a completely disordered structure is formed without the help of F127.

The structural study is further carried out by the TEM measurements for phenol–formaldehyde mesoporous carbons. As shown in Fig. 3a, ordered mesoporous structure and disordered mesoporous structure are both observed in BMC, which is in good agreement with the XRD pattern shown in Fig. 2. The ordered pores (about 3.5 nm, Fig. 3b) are created by the assembly of F127, which are similar to the typical cubic mesoporous carbon OMC as shown in Fig. 3c, and the disordered pores (Fig. 3b) are introduced by SiO_2 particles. Meanwhile, only disordered pores with a wide pore size distribution are obtained for DMC (Fig. 3d), which can be attributed to the aggregation of SiO_2 particles during the synthesized process.

The FTIR spectra of BMC, OMC and DMC are shown in Fig. 4. The major features of the spectra of these carbons are similar with bands at 1128 cm^{-1} and a broad band at around 3432 cm^{-1} which is mainly caused by the O–H stretching vibration of the absorbed water molecules. The band at 1128 cm^{-1} is caused by the stretching vibration of the C–O bonds. In addition, the C=O stretching vibrations related to carbonyl and/or carboxyl groups can be found at around 1730 cm^{-1} for all three products. Meanwhile, the band at 1260 cm^{-1} which can be assigned tentatively to C–O–C vibrations in ether structures or other single bonded oxo group C–O–R and very weak bands centered near 2300 cm^{-1} assigned to C–O groups due to ketone are found for these mesoporous carbons [29,32]. It is necessary to note that the absorption bands at 1410 cm^{-1} of BMC and DMC are much stronger than that of OMC due to their lactone structure introduced during the NaOH treatment [32]. The modification of the samples can significantly affect the surface functionality.

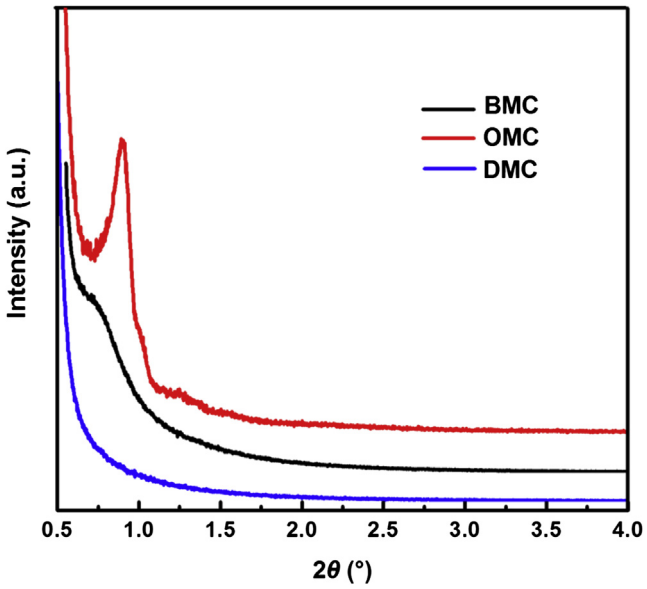

Fig. 2. Small-angle XRD patterns for BMC, OMC and DMC.

The specific surface area and pore size distribution analyses of BMC, OMC and DMC conducted using N_2 adsorption and desorption experiments are shown in Fig. 5. The OMC sample shows typical type IV curves with an H_2-type hysteresis loop implying a cage-like mesopore. The diameter of these pores is calculated to be 3.2 nm by the Barrett–Joyner–Halenda (BJH) method (see the inset in Fig. 5) with surface area of 408 $m^2\ g^{-1}$. The DMC sample with surface area of 464 $m^2\ g^{-1}$ shows the hysteresis loop at relative pressure of ca. 0.7. A sharp capillary condensation step is also shown at high relative pressures which indicating the obvious aggregation of SiO_2 particles is carried out without the help of F127. The BMC sample shows much larger BET surface area (722 $m^2\ g^{-1}$) than both the OMC and DMC samples, and exhibits two hysteresis loop at relative pressures of ca. 0.4 and 0.7 in its N_2 adsorption–desorption isotherm, demonstrating that BMC has two types of mesopores: cage-like pores in the OMC matrix (about 3.5 nm) and SiO_2-templating mesopores (about 7.0 nm), which meet the pore sizes of OMC and DMC very well. It should be noted that there are a very small amount of mesopores about 12–20 nm in the BMC (see the inset in Fig. 5), demonstrating that only slight aggregation of SiO_2 particles can happen. These above results are in agreement with the TEM observations (Fig. 3). As a result, BMC not only exhibits higher surface area but also keep the mesoporous structures of OMC and DMC at the same time.

3.2. Electrochemical test

Fig. 6a shows the cyclic voltammograms (CVs) of the BMC electrode at scan rates of 1–50 mV s^{-1} between −0.1 V and 0.7 V (vs. Ag/AgCl) in H_2SO_4 aqueous (1 M) electrolyte. There is no obvious distortion in the CV curves when the sweep rate is

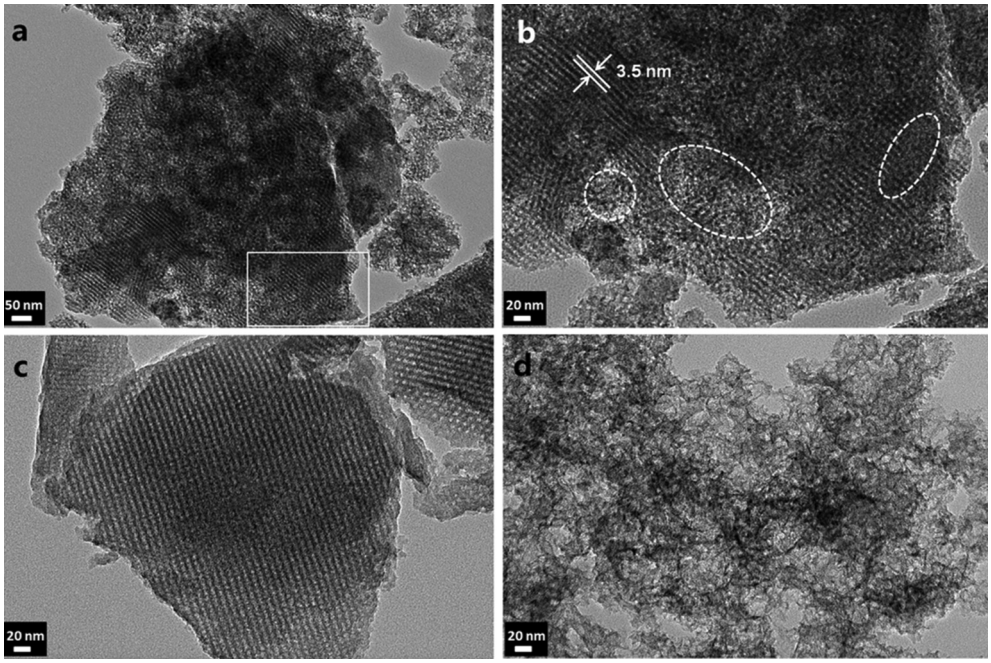

Fig. 3. (a) TEM image of BMC and (b) is the high-resolution image of the selected area in image (a); (c) and (d) TEM images of OMC and DMC, respectively.

increased in the range of 1 mV s^{-1}–20 mV s^{-1} which suggesting a highly reversible system can be employed in H_2SO_4 electrolyte within the potential range. However, the distortion becomes sharp when the scan rate reaches 50 mV s^{-1}, which reflecting a more significant ohmic resistance in pores. The CVs of BMC, OMC and DMC electrodes at the same sweep rate of 1 mV s^{-1} are shown in Fig. 6b. The CV curves of all these three electrodes are deviated from idealized double-layer behaviors with a pair of broad and reversible faradaic surface redox reactions, behaving as pseudocapacitances. These peaks are attributed to the redox reactions of the O-containing (C═O, C–OR) and N-containing surface functionalities on the surface of phenol–formaldehyde carbon after acid-treatment as reported previously [31,33,34]. It should be noted that BMC and OMC exhibit redox reactions peaks different from that of OMC, which can be attributed to their functional groups intruded during alkaline wash. Moreover, it is clear that the BMC electrode exhibits a much higher specific capacitance compared with the OMC and DMC electrodes.

The galvanostatic charge/discharge curves of the BMC were measured at 0.1–10 A g^{-1}, as shown in Fig. 6c. The charge curves are symmetrical to their discharge counterparts, revealing a good capacitive behavior and electrochemical reversibility. In addition, compared with the OMC and DMC electrodes, the BMC electrode exhibits larger capacitance (see the inset in Fig. 6c) due to its larger surface area. For instance, the BMC electrode delivers a specific capacitance of 344 F g^{-1} at the current density of 0.1 A g^{-1}, which is over 1.5 times larger than that of the OMC (219 F g^{-1}) and DMC (224 F g^{-1}) electrodes. Specific capacitance as a function of currents for the BMC, OMC and DMC electrodes are shown in Fig. 6d. It is

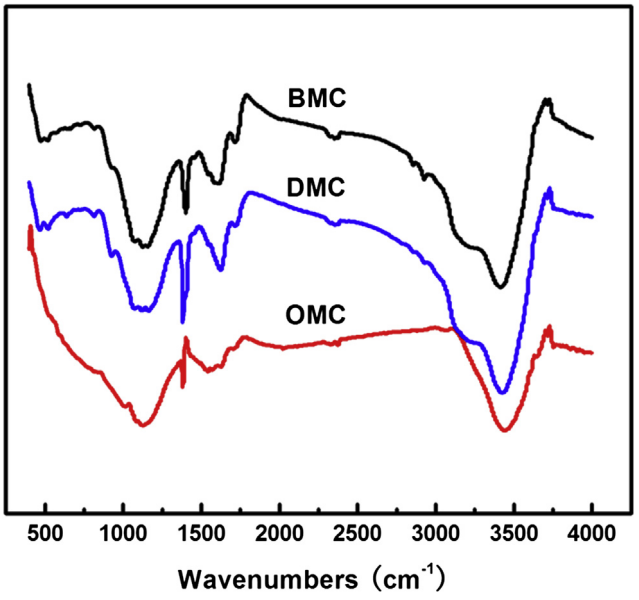

Fig. 4. FTIR spectra of BMC, OMC and DMC.

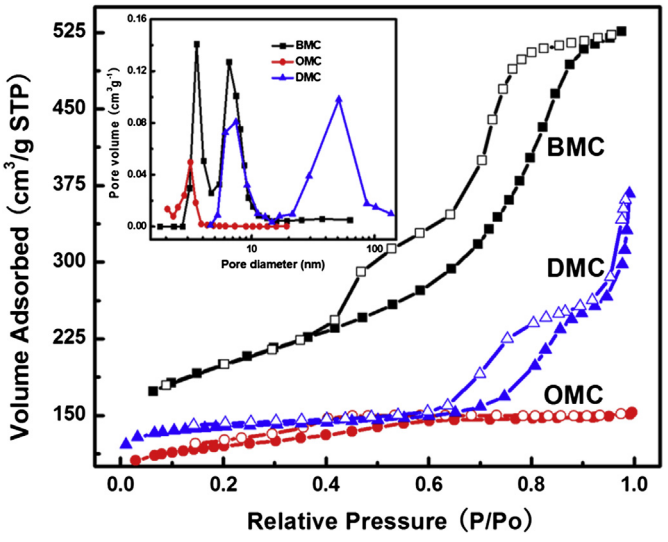

Fig. 5. N_2 adsorption–desorption isotherms of the BMC, OMC and DMC, inset showing the corresponding pore size distribution.

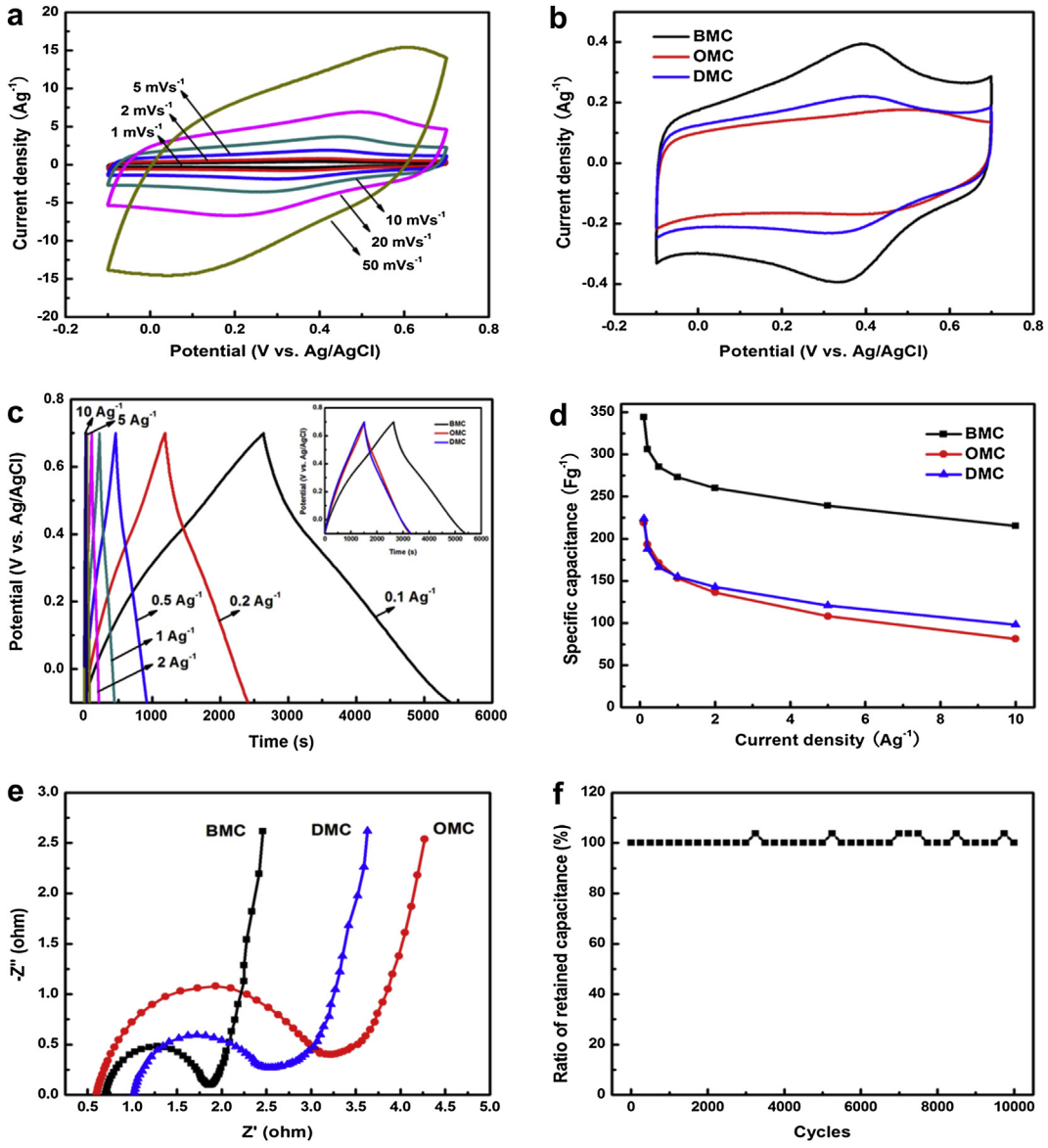

Fig. 6. (a) CVs of the BMC electrodes with different sweep rate; (b) CVs of the BMC, OMC and DMC electrodes at the same sweep rate of 1 mV s^{-1}; (c) galvanostatic charge/discharge curves of the BMC electrodes with different current densities, inset shows galvanostatic charge/discharge comparison of the BMC, OMC and DMC electrodes at the same current density of 0.1 A g^{-1}; (d) specific capacitance as a function of currents for the BMC, OMC and DMC electrodes; (e) impedance Nyquist plots of the BMC, OMC and DMC electrodes; (f) cyclability test of the BMC electrode at a current density of 1 A g^{-1}.

clearly shown that specific capacitances of these electrodes are decreased with the increase of current density. Therefore, the BMC, OMC and DMC electrodes can remain 63%, 37% and 44% of the specific capacitances when charge/discharge at a high-rate of 10 A g^{-1}, respectively. The higher specific capacitance at low-rate and better rate capability at high-rate of the BMC electrode can be ascribed to its unique mesoporous structure. The ordered mesoporous about 3.5 nm provide channels among these disordered mesoporous about 7.0 nm. As a result, the electrolyte can diffuse into the inner pores of the BMC particles through these channels leading to a larger specific capacitance at low-rate. Meanwhile, the disordered mesoporous can still achieve efficient electrolyte diffusion pathways at high-rate for their larger pore size, so that better rate capability can be obtained.

Electrochemical impedance spectroscopy (EIS) has been used to investigate the performance of electrochemical capacitors such as internal resistance, capacity, etc. Fig. 6e shows the relation between Z″ (imaginary) and Z′ (real) impedance components of electrochemical capacitors based on BMC, OMC and DMC electrode materials, respectively. All the spectra show a semicircle at the high–medium frequency and vertical lines at low frequency region. The semicircle curves depict a typical electric double-layer behavior while the vertical lines reveal the supercapacitive behavior. The diameters of the semicircle reflect charge transfer resistance which is strongly dependent on the abilities of ion transfer and electron conduction [35,36]. It can be observed that the charge transfer resistances decrease in the sequence of OMC > DMC > BMC as revealed by the semicircle, which clearly shows that the BMC electrode provide easier access (less resistance) for intercalation and deintercalation of charges compared to the OMC and DMC electrodes.

Long cycling life is an important requirement for supercapacitor electrodes. The cycle stability of the BMC electrode was evaluated at the current density of 1 A g^{-1} between −0.1 V and 0.7 V for 10,000

cycles. The capacitance retention ratio as a function of cycle number is displayed in Fig. 6f. After 10,000 continuous cycles, the BMC electrode displays excellent long cycle life along with less than 1% decay, demonstrating the superior long-term electrochemical stability, which is significant for the practical application.

4. Conclusion

We develop a facile approach to prepare bimodal mesoporous phenol–formaldehyde carbon by EISA with resol, F127 and SiO_2 particles. The obtained unique bimodal mesoporous carbon (BMC) materials consist of ordered mesostructure of narrow pore sizes (3.5 nm), and disordered mesostructure with pore size of 7.0 nm. The ordered mesopores provide channels and connect those disordered mesopores together. As the result, the unique bimodal mesoporous structure contributes to attractive capabilities as a promising material in energy storage: the disordered mesoporous connected together provide a favorable ion path for electrolyte penetration and allow the ionic transport fast into the bulk of the BMC particles, which lead to good electronic conductivity. So that excellent capacitance retention at high-rate for pulse power applications can be obtained. At the same time, the ordered mesopores allow the produced BMC to exhibit a specific surface area up to 722 $m^2\ g^{-1}$ and a specific capacitance up to 344 F g^{-1}. Furthermore, the BMC electrode shows an excellent stability of less than 1% decay in specific capacitance after 10,000 cycles. All these results indicate that the bimodal mesoporous carbon material is a promising candidate for high-performance supercapacitors.

Acknowledgment

This work was supported by the National Natural Science Foundation of China (No. 21274043).

References

[1] M. Winter, R.J. Brodd, Chem. Rev. 104 (2004) 4245.
[2] S.L. Xiong, C.Z. Yuan, X.G. Zhang, B.J. Xi, Y.T. Qian, Chem. Eur. J. 15 (2009) 5320.
[3] B.E. Conway, Electrochemical Supercapacitors Scientific Fundamentals and Technological Applications, Kluwer Academic/Plenum Publishers, New York, USA, 1999.
[4] Z.S. Wu, D.W. Wang, W.C. Ren, J.P. Zhao, G.M. Zhou, F. Li, H.M. Cheng, Adv. Funct. Mater. 20 (2010) 3595.
[5] J.W. Lang, L.B. Kong, W.J. Wu, Y.C. Luo, L. Kang, Chem. Commun. 35 (2008) 4213.
[6] Y.H. Lin, T.Y. Wei, H.C. Chien, S.Y. Lu, Adv. Energy Mater. 1 (2011) 901.
[7] S.W. Woo, K. Dokko, H. Nakano, K. Kanamura, J. Mater. Chem. 18 (2008) 1674.
[8] H. Nakagawa, A. Shudo, K. Miura, J. Electrochem. Soc. 147 (2000) 38.
[9] M. Anouti, L. Timperman, M. Hilali, A. Boisset, H. Galiano, J. Phys. Chem. C 116 (2012) 9412.
[10] H.L. Lu, W.J. Dai, M.B. Zheng, N.W. Li, G.B. Ji, J.M. Cao, J. Power Sources 209 (2012) 243.
[11] Z. Li, L. Zhang, B.S. Amirkhiz, X.H. Tan, Z.W. Xu, H.L. Wang, B.C. Olsen, C.M.B. Holt, D. Mitlin, Adv. Energy Mater. 2 (2012) 431.
[12] L.L. Zhang, X.S. Zhao, Chem. Soc. Rev. 38 (2009) 2520.
[13] M. Rose, Y. Korenblit, E. Kockrick, L. Borchardt, M. Oschatz, S. Kaskel, G. Yushin, Small 7 (2011) 1108.
[14] Y.K. Lv, L.H. Gan, M.X. Liu, W. Xiong, Z.J. Xu, D.Z. Zhu, D.S. Wright, J. Power Sources 209 (2012) 152.
[15] H.J. Liu, J. Wang, C.X. Wang, Y.Y. Xia, Adv. Energy Mater. 1 (2011) 1101.
[16] K.S. Xia, Q.M. Gao, J.H. Jiang, J. Hu, Carbon 46 (2008) 1718.
[17] J.W. Lang, X.B. Yan, X.Y. Yuan, J. Yang, Q.J. Xue, J. Power Sources 196 (2011) 10472.
[18] J.W. Lang, X.B. Yan, W.W. Liu, R.T. Wang, Q.J. Xue, J. Power Sources 204 (2012) 220.
[19] D.W. Wang, F. Li, M. Liu, G.Q. Lu, H.M. Cheng, Angew. Chem. Int. Ed. 47 (2008) 373.
[20] D. Banham, F.X. Feng, J. Burt, E. Alsrayheen, V. Birss, Carbon 48 (2010) 1056.
[21] A.H. Lu, W. Schmidt, B. Spliethoff, F. Schüth, Adv. Mater. 15 (2003) 1602.
[22] W.J. Gao, Y. Wan, Y.Q. Dou, D.Y. Zhao, Adv. Energy Mater. 1 (2011) 115.
[23] Y.R. Liang, D.C. Wu, R.W. Fu, Langmuir 25 (2009) 7783.
[24] G.H. Sun, K.X. Li, L.J. Xie, J.L. Wang, Y.Q. Li, Microporous Mesoporous Mater. 151 (2012) 282.
[25] B. You, J. Yang, Y.Q. Sun, Q.D. Su, Chem. Commun. 47 (2011) 12364.
[26] Y. Meng, D. Gu, F.Q. Zhang, Y.F. Shi, H.F. Yang, Z. Li, C.Z. Yu, B. Tu, D.Y. Zhao, Angew. Chem. Int. Ed. 44 (2005) 7053.
[27] Y. Meng, D. Gu, F.Q. Zhang, Y.F. Shi, L. Cheng, D. Feng, Z.X. Wu, Z.X. Chen, Y. Wan, A. Stein, D.Y. Zhao, Chem. Mater. 18 (2006) 4447.
[28] Y. Huang, H.Q. Cai, T. Yu, F.Q. Zhang, F. Zhang, Y. Meng, D. Gu, Y. Wan, X.L. Sun, B. Tu, D.Y. Zhao, Angew. Chem. Int. Ed. 46 (2007) 1089.
[29] P.A. Bazula, A.H. Lu, J.J. Nitz, F. Schüth, Microporous Mesoporous Mater. 108 (2008) 266.
[30] F. Lufrano, P. Staiti, Energy Fuels 24 (2010) 3313.
[31] T.W. Cai, M. Zhou, D.Y. Ren, G.S. Han, S.Y. Guan, J. Power Sources 231 (2013) 197.
[32] J.W. Shim, S.J. Park, S.K. Ryu, Carbon 39 (2001) 1635.
[33] M.P. Bichat, E.R. Piñero, F. Béguin, Carbon 48 (2010) 4351.
[34] V. Khomenko, E.R. Piñero, F. Béguin, J. Power Sources 195 (2010) 4234.
[35] G.W. Sun, J.T. Wang, X.J. Liu, D.H. Long, W.M. Qiao, L.C. Ling, J. Phys. Chem. C 114 (2010) 18745.
[36] W. Sugimoto, H. Iwata, K. Yokoshima, Y. Murakami, Y. Takasu, J. Phys. Chem. B 109 (2005) 7330.